4890 *Chem. Mater.* **2010,** *22,* 4890–4895
DOI:10.1021/cm101677x

CHEMISTRY OF
MATERIALS
Article

Synthesis and Photovoltaic Properties of Donor−Acceptor Copolymers Based on 5,8-Dithien-2-yl-2,3-diphenylquinoxaline

Erjun Zhou,[†] Junzi Cong,[†] Keisuke Tajima,[†] and Kazuhito Hashimoto*,[†,‡]

[†]*HASHIMOTO Light Energy Conversion Project, ERATO, Japan Science and Technology Agency (JST), and* [‡]*Department of Applied Chemistry, School of Engineering, The University of Tokyo, 7-3-1 Hongo, Bunkyo-ku, Tokyo 113-8656, Japan*

Received June 16, 2010. Revised Manuscript Received July 22, 2010

Four donor−acceptor (D−A) type copolymers, namely, poly{9,9-dioctylfluorene-2,7-diyl-*alt*-5,8-dithien-2-yl-2,3-diphenylquinoxaline-5′,5′′-diyl} (**PF-DTQx**), poly{*N*-[1-(2′-ethylhexyl)-3-ethylheptanyl]carbazole-2,7-diyl-*alt*-5,8-dithien-2-yl-2,3-diphenylquinoxaline-5′,5′′-diyl} (**PC-DTQx**), poly{5,11-di(1-decylundecyl)indolo[3,2-b]carbazole-3,9-diyl-*alt*-5,8-dithien-2-yl-2,3-diphenylquinoxaline-5′,5′′-diyl} (**PIC-DTQx**), and poly{N-[1-(2′-ethylhexyl)-3-ethylheptanyl]-dithieno[3,2-b:2′,3′-d]-pyrrole-2,6-diyl-*alt*-5,8-dithien-2-yl-2,3-diphenylquinoxaline-5′,5′′-diyl} (**PDTP-DTQx**), were synthesized by Suzuki or Stille coupling reactions. By changing the donor segment, the band gaps and energy levels of these 5,8-dithien-2-yl-2,3-diphenylquinoxaline (DTQx)-based polymers could be finely tuned. PDTP-DTQx exhibited the narrowest band gap of 1.56 eV and the absorption edge extended to 770 nm. We investigated bulk heterojunction type polymer solar cells (PSCs) based on these copolymers as the electron donor materials, and [6,6]-phenyl C_{61} butyric acid methyl ester (PCBM) or [6,6]-phenyl C_{71} butyric acid methyl ester ($PC_{70}BM$) as the acceptor. The power conversion efficiency (PCE) of the PSCs was in the range of 1.17−3.23% under AM 1.5 illumination (100 mW/cm^2).

Introduction

Donor−acceptor (D−A) type alternating copolymers with an electron-rich unit (donor) and an electron-deficient unit (acceptor) in the polymer backbone have recently drawn much attention for application to many optoelectronic devices such as polymer light-emitting diodes (PLEDs), field-effect transistors (FETs), sensors, photodetectors, and polymer solar cells (PSCs).[1] This D−A approach for designing the polymers is highly effective for tuning physical properties such as solubility, band gap, energy levels, and carrier mobility by choosing a suitable combination from the vast variety of donor and acceptor segments available.[2] These physical properties, especially the absorption spectra and the energy levels, are critical for realizing highly efficient PSCs in terms of spectral matching to the solar spectrum and charge separation efficiency at the material interfaces. Thus, many novel conjugated polymers have been synthesized relying on this strategy and used in PSCs to reach power conversion efficiency (PCE) of > 6%.[3]

Among the wide variety of acceptor segments, 4,7-dithien-2-yl-2,1,3-benzothiadiazole (DTBT) has been copolymerized with almost all available donor segments including pyrrole,[4] didecyloxyphenylene,[5] fluorene,[6] carbazole,[7] silafluorene (or dibenzosilole),[8] indeno[2,1-a]indene,[9] cyclopenta[2,1-b:3,4-b]dithiophene,[10] dithienosilole,[11] dithieno[3,2-*b*:2′,3′-*d*]pyrrole,[12] indolo[3,2-b]carbazole,[13]

---

*Corresponding author. E-mail: hashimoto@light.t.u-tokyo.ac.jp.

(1) (a) Burroughes, J. H.; Bradley, D. D. C.; Brown, A. B.; Marks, R. N.; Mackay, K.; Friend, R. H.; Burn, P. L.; Holmes, A. B. *Nature* **1990**, *347*, 539. (b) Sirringhaus, H.; Tessler, N.; Friend, R. H. *Science* **1998**, *280*, 1741. (c) Chen, L. H.; McBranch, D. W.; Wang, H.-L; Helgeson, R.; Wudl, F.; Whitten, D. G. *Proc. Natl. Acad. Sci. U.S.A.* **1999**, *96*, 12287. (d) Yu, G.; Wang, J.; McElvain, J.; Heeger, A. *J. Adv. Mater.* **1998**, *10*, 1431. (e) Yu, G.; Hummelen, J.; Wudl, F.; Heeger, A. J. *Science* **1995**, *270*, 1789.

(2) (a) Roncali, J. *Chem. Rev.* **1997**, *97*, 173. (b) Ajayaghosh, A. *Chem. Soc. Rev.* **2003**, *32*, 181.

(3) (a) Peet, J.; Kim, J. Y.; Coates, N. E.; Ma, W. L.; Moses, D.; Heeger, A. J.; Bazan, G. C. *Nat. Mater.* **2007**, *6*, 497. (b) Hou, J. H.; Chen, H. Y.; Zhang, S. Q.; Li, G.; Yang, Y. *J. Am. Chem. Soc.* **2008**, *130*, 16144. (c) Liang, Y. Y.; Feng, D. Q.; Wu, Y.; Tsai, S.-T.; Li, G.; Ray, C.; Yu, L. P. *J. Am. Chem. Soc.* **2009**, *131*, 7792. (d) Park, S. H.; Roy, A.; Beaupré, S.; Cho, S.; Coates, N.; Moon, J. S.; Moses, D.; Leclerc, M.; Lee, K.; Heeger, A. J. *Nat. Photonics* **2009**, *3*, 297. (e) Chen, H.-Y.; Hou, J. H.; Zhang, S. Q.; Liang, Y. Y.; Yang, G. W.; Yang, Y.; Yu, L. P.; Wu, Y.; Li, G. *Nat. Photonics* **2009**, *3*, 649.

(4) (a) Dhanabalan, A.; van Duren, J. K. J.; van Hal, P. A.; van Dongen, J. L. J.; Janssen, R. A. J. *Adv. Funct. Mater.* **2001**, *11*, 255–262. (b) Brabec, C. J.; Winder, C.; Sariciftci, N. S.; Hummelen, J. C.; Dhanabalan, A.; van Hal, P. A.; Janssen, R. A. J. *Adv. Funct. Mater.* **2002**, *12*, 709.

(5) Liu, C. L.; Tsai, J. H.; Lee, W. Y.; Chen, W. C.; Jenekhe, S. A. *Macromolecules* **2008**, *41*, 6952.

(6) (a) Svensson, M.; Zhang, F. L.; Veenstra, S. C.; Verhees, W. J. H.; Hummelen, J. C.; Kroon, J. M.; Inganäs, O.; Andersson, M. R. *Adv. Mater.* **2003**, *15*, 988. (b) Chen, M. -H.; Hou, J. H.; Hong, Z. R.; Yang, G. W.; Sista, S.; Chen, L.-M.; Yang, Y. *Adv. Mater.* **2009**, *21*, 4238.

(7) (a) Blouin, N.; Michaud, A.; Leclerc, M. *Adv. Mater.* **2007**, *19*, 2295. (b) Chu, T.-Y; Alem, S.; Verly, P. G.; Wakim, S.; Lu, J. P.; Tao, Y.; Beaupré, S.; Leclerc, M.; Bélanger, F.; Désilets, D.; Rodman, S.; Waller, D.; Gaudiana, R. *Appl. Phys. Lett.* **2009**, *95*, 063304.

(8) (a) Boudreault, P. T.; Michaud, A.; Leclerc, M. *Macromol. Rapid Commun.* **2007**, *28*, 2176. (b) Wang, E. G.; Wang, L.; Lan, L. F.; Luo, C.; Zhuang, W. L.; Peng, J. B.; Cao, Y. *Appl. Phys. Lett.* **2008**, *92*, 033307.

(9) Song, S.; Jin, Y.; Kim, S. H.; Moon, J.; Kim, K.; Kim, J. Y.; Park, S. H.; Lee, K.; Suh, H. *Macromolecules* **2008**, *41*, 7296.

Scheme 1. Synthetic Route for the Monomer

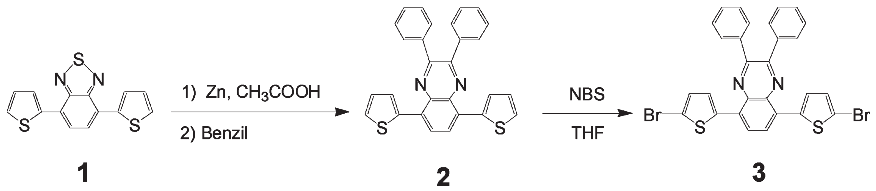

benzo[2,1-b:3,4-b′]dithiophene,[14] benzo[1,2-b:4,5-b′]dithiophene,[15] indeno[1,2b]fluorene,[16] ladder-type oligo-*p*-phenylene,[17] and germafluorene.[18] When these materials were applied to PSCs, PCEs in the range of 0.41−6.1% were achieved. Because PSC performance strongly depends on the choice of the donor segment, the development of novel and versatile building blocks such as DTBT and systematic investigation of D−A type polymers are important areas of research in the search for photovoltaic polymers with superior properties.

Quinoxaline-based polymers have shown interesting optoelectronic properties and considerable promise for the design of D−A type photovoltaic polymers.[19] In this study, we investigate the combination of the 5,8-dithien-2-yl-2,3-diphenylquinoxaline (DTQx) acceptor segment with three well-known donor segments, namely, carbazole, indolo[3,2-b]carbazole, and dithieno[3,2-b:2′,3′-d]pyrrole. These three donor segments contain nitrogen atoms, which have strong electron-donating ability. The copolymer of DTQx and fluorene, which has been reported to give high photovoltaic performance,[19f,g] was also synthesized for comparison. The structural similarity of DTQx to DTBT provides similar versatility as a building block for use in the coupling polymerization reactions. The effects of the different donor segments on the absorption spectra, energy levels and the photovoltaic performance of the resulting DTQx-containing D−A copolymers were investigated in detail.

Results and Discussion

Material Synthesis. The monomer **3**, 5,8-di(2-bromothien-5-yl)-2,3-diphenylquinoxaline, was synthesized according to a modified literature procedure,[19a] as shown in Scheme 1. The synthetic routes for preparing the four DTQ-based polymers are shown in Scheme 2. Three types of DTQx-based copolymers, PF-DTQx, PC-DTQx, and PIC-DTQx, were synthesized by the Suzuki coupling reaction between **3** and the corresponding boronic esters of the donor segments. PDTP-DTQx was synthesized by the Stille coupling reaction between **3** and the bisstannyl derivative of dithieno[3,2-b:2′,3′-d]pyrrole. For the synthesis of PF-DTQx and PC-DTQx, the feed molar ratios of the donor and the acceptor monomers was set to 100:95 to avoid the formation of a large insoluble fraction of the polymers. As a result, all the polymers have good solubility in chloroform (CF), chlorobenzene (CB), and 1,2-dichlorobenzene (DCB), and their number-average molecular weights (M_n) and the polydispersity indices were in the range of 8.1−21.1 K and 1.4−1.9, respectively.

Optical and Electrochemical Properties. The normalized UV−vis absorption spectra of the four copolymers in $CHCl_3$ solutions are shown in Figure 1. The peak at the longer wavelength can be attributed to intramolecular charge-transfer (ICT) transitions. PF-DTQx, PC-DTQx, and PIC-DTQx show similar absorption spectra with absorption maxima at 524, 517, and 514 nm, respectively. The slight blue shift for PC-DTQx and PIC-DTQx, compared with PF-DTQx, is likely because of the larger steric hindrance of the side chains in these two polymers. In contrast, the absorption band of PDTP-DTQx (617 nm) is at a considerably longer wavelength compared with the absorptions bands of the other two copolymers. This change in the absorption is similar to the cases of DTBT-based copolymers; PF-DTBT, PC-DTBT and PIC-DTBT have absorption maxima at 537, 545, and 531 nm, respectively,[20] but the absorption peak of PDTP-DTBT extends to 671 nm.[12]

---

(10) Moulé, A. J.; Tsami, A.; Bünnagel, T. W.; Forster, M.; Kronenberg, N. M.; Scharber, M.; Koppe, M.; Morana, M.; Brabec, C. J.; Meerholz, K.; Scherf, U. *Chem. Mater.* **2008**, *20*, 4045.

(11) (a) Liao, L.; Dai, L. M.; Smith, A.; Durstock, M.; Lu, J. P.; Ding, J. F.; Tao, Y. *Macromolecules* **2007**, *40*, 9406. (b) Huo, L. J.; Chen, H.-Y.; Hou, J. H.; Chen, T. L.; Yang, Y. *Chem. Commun.* **2009**, 5570.

(12) Zhou, E. J.; Nakamura, M.; Nishizawa, T.; Zhang, Y.; Wei, Q. S.; Tajima, K.; Yang, C. H.; Hashimoto, K. *Macromolecules* **2008**, *41*, 8302.

(13) Zhou, E. J.; Yamakawa, S.; Tajima, K.; Yang, C. H.; Hashimoto, K. *J. Mater. Chem.* **2009**, *19*, 7730.

(14) Zhou, H. X.; Yang, L. Q.; Xiao, S. Q.; Liu, S. B.; You, W. *Macromolecules* **2010**, *43*, 811.

(15) Huo, L. J.; Hou, J. H.; Zhang, S. Q.; Chen, H.-Y.; Yang, Y. *Angew. Chem., Int. Ed.* **2010**, *49*, 1500.

(16) Kim, J. K.; Kim, S. H.; Jung, I. H.; Jeong, E.; Xia, Y. J.; Cho, S.; Hwang, I.-W.; Lee, K.; Suh, H.; Shim, H.-K.; Woo, H. Y. *J. Mater. Chem.* **2010**, *20*, 1577.

(17) Zheng, Q. D.; Jung, B. J.; Sun, J.; Katz, H. E. *J. Am. Chem. Soc.* **2010**, *132*, 5394.

(18) Allard, N.; Aïch, R. B.; Gendrom, D.; Boudreault, P. T.; Tessier, C.; Alem, S.; Tse, S.-C.; Tao, Y.; Leclerc, M. *Macromolecules* **2010**, *43*, 2328.

(19) (a) Gadisa, A.; Mammo, W.; Andersson, L. M.; Admassie, S.; Zhang, F. L.; Andersson, M. R.; Inganäs, O. *Adv. Funct. Mater.* **2007**, *17*, 3836. (b) Huo, L. J.; Tan, Z. A.; Wang, X.; Zhou, Y.; Han, M. F.; Li, Y. F. *J. Polym. Sci., Part A: Polym. Chem.* **2008**, *46*, 4038. (c) Blouin, N.; Michaud, A.; Gendron, D.; Wakim, S.; Blair, E.; Neagu-Plesu, R.; Belletête, M.; Durocher, G.; Tao, Y.; Leclerc, M. *J. Am. Chem. Soc.* **2008**, *130*, 732. (d) Günes, S.; Baran, D.; Günbas, G.; özyurt, F.; Fuchsbauer, A.; Sariciftci, N. S.; Toppare, L. *Sol. Energy Mater. Sol. Cells* **2008**, *92*, 1162. (e) Yu, C.-Y.; Chen, C.-P.; Chan, G.-H.; Hwang, G.-W.; Ting, C. *Chem. Mater.* **2009**, *21*, 3262. (f) Lindgren, L. J.; Zhang, F. L.; Andersson, M.; Barrau, S.; Hellström, S.; Mammo, W.; Perzon, E.; Inganäs, O.; Andersson, M. R. *Chem. Mater.* **2009**, *21*, 3491. (g) Kitazawa, D.; Watamabe, N.; Yamamoto, S.; Tsukamoto, J. *Appl. Phys. Lett.* **2009**, *95*, 053701. (h) Lee, J.-Y.; Shin, W.-S.; Haw, J.-R.; Moon, D.-K. *J. Mater. Chem.* **2009**, *19*, 4938. (i) Peng, Q.; Xu, J.; Zhang, W. X. *J. Polym. Sci., Part A: Polym. Chem.* **2009**, *47*, 3399. (j) Tsimi, A.; Bünnagel, T. W.; Farrell, T.; Scharber, M.; Choulis, S. A.; Brabec, C. J.; Scherf, U. *J. Mater. Chem.* **2007**, *17*, 1353.

(20) Zhou, E. J.; Cong, J. Z.; Yamakawa, S.; Wei, Q. S.; Nakamura, M.; Tajima, K.; Yang, C. H.; Hashimoto, K. *Macromolecules* **2010**, *43*, 2873.

Scheme 2. Synthetic Routes for the Four DTQx-Based Donor−Acceptor Type Copolymers

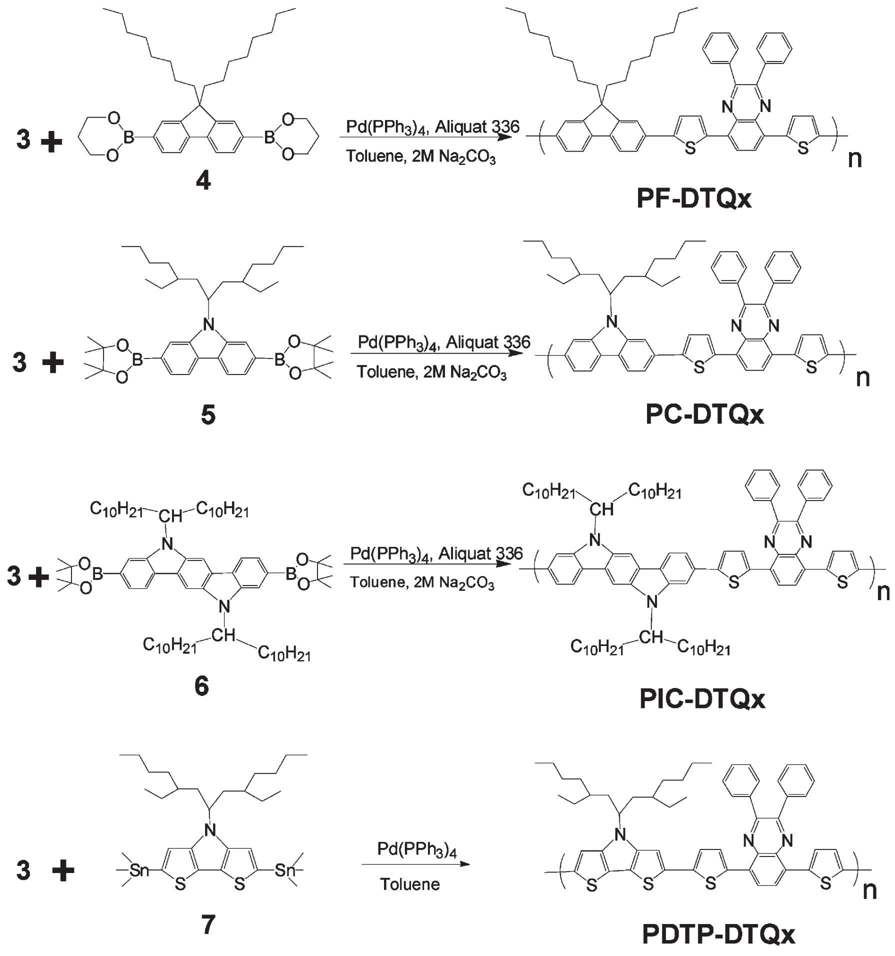

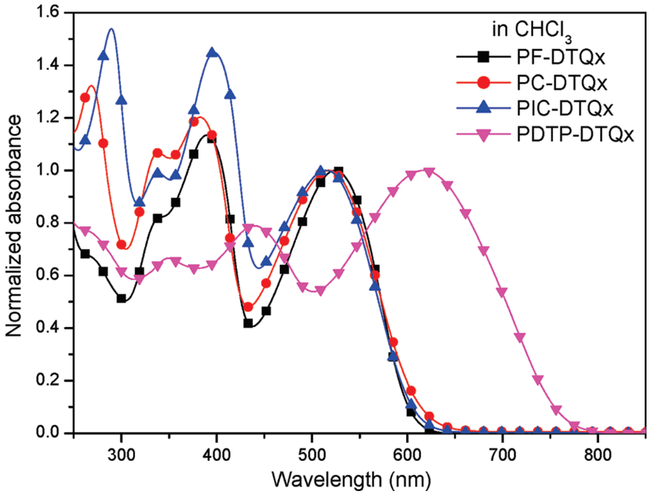

Figure 1. Normalized absorption spectra of the copolymers in $CHCl_3$ solution.

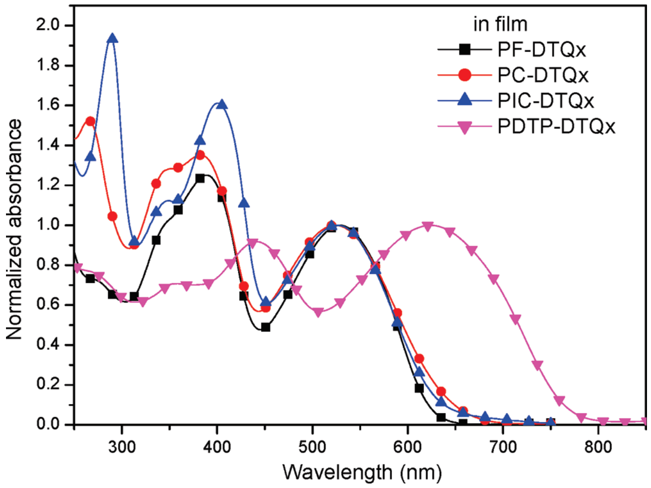

Figure 2. Normalized absorption spectra of the copolymer films on quartz plates.

The absorption spectra of the polymer films are shown in Figure 2. The absorption maxima of the polymer films are slighted red-shifted by 4−13 nm compared with those of the polymer solutions, indicating that the intermolecular interaction in the solid state was restricted by the large steric hindrance of both the alkyl chains in the donor segments and the diphenyl group in the quinoxaline segment. The optical band gaps (E_g^{opt}) of the four polymers are estimated from the absorption onset and summarized in Table 1.

In addition to the absorption properties, the highest occupied molecular orbital (HOMO) and lowest unoccupied molecular orbital (LUMO) energy levels of the conjugated polymers are key parameters that influence

Table 1. Optical and Electrochemical Properties of DTQx-Based Polymers

	UV−vis absorption spectrum				cyclic voltammogram				
	in $CHCl_3$	in film			p-doping		n-doping		
polymer	λ_{max} (nm)	λ_{max} (nm)	λ_{onset} (nm)	E_g^{opt} (eV)	E_{on}^{ox} (V)	HOMO (eV)	E_{on}^{red} (V)	LUMO (eV)	E_g^{EC} (eV)
PF-DTQx	524	528	625	1.98	0.69	−5.49	−1.37	−3.43	2.06
PC-DTQx	517	524	635	1.95	0.62	−5.42	−1.36	−3.44	1.98
PIC-DTQx	514	527	650	1.91	0.73	−5.53	−1.26	−3.54	1.99
PDTP-DTQx	617	624	770	1.61	0.24	−5.04	−1.32	−3.48	1.56

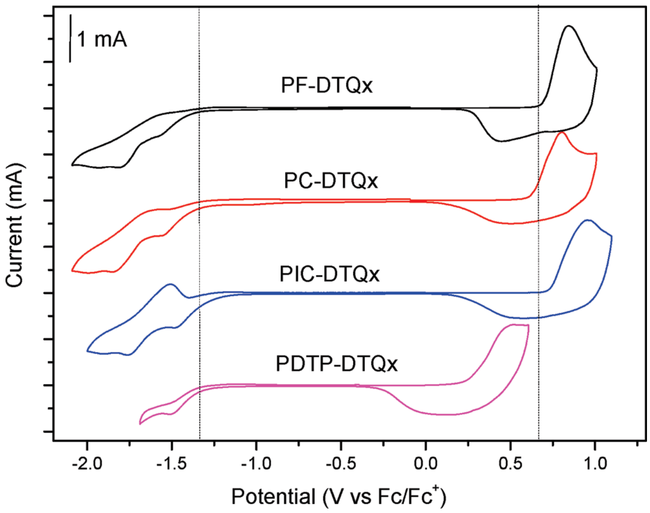

Figure 3. Cyclic voltammograms of the polymers films deposited on a platinum plate in an acetonitrile solution of 0.1 M $[Bu_4N]PF_6$ (Bu = butyl) at a scan rate of 50 mV/s.

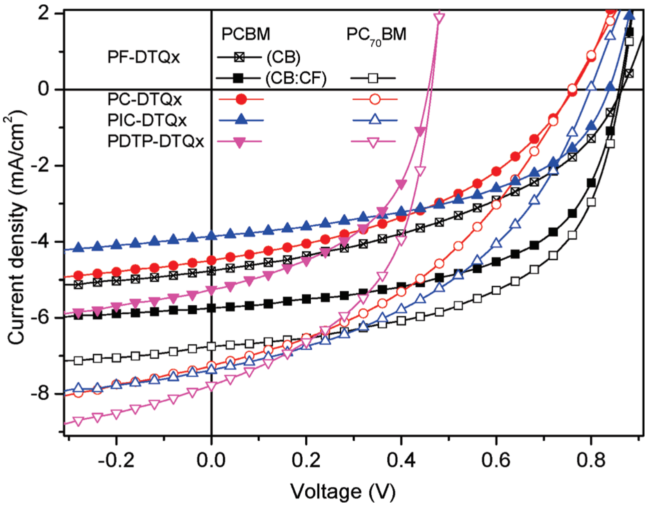

Figure 4. *I*−*V* curves of the polymer solar cells based on the DTQx-based polymers under AM 1.5 illumination (100 mW/cm^2).

the overall performance of the photovoltaic device through the efficiency of charge separation and the open-circuit voltage (V_{OC}). Cyclic voltammetry (CV) was used to determine the energy levels of the DTQx-based conjugated polymers (see Figure 3).[21] CV curves were recorded in referenced to an Ag/Ag$^+$ (0.01 M $AgNO_3$ in acetonitrile) electrode and calibrated by the ferrocene−ferrocenium (Fc/Fc$^+$) redox couple (4.8 eV below the vacuum level). From the onset oxidation potential (E_{on}^{ox}) and onset reduction potential (E_{on}^{red}) of the polymers, the HOMO and LUMO energy levels as well as the electrochemical band gaps (E_g^{EC}) were calculated (Table 1). The electrochemical band gap E_g^{EC} coincides with the optical band gap estimated from the UV−vis absorption onset for each of the copolymers within the experimental error. All the DTQx-based polymers had similar LUMO energy levels at −3.43 to −3.48 eV. The HOMO energy level of PDTP-DTQx was shifted upward by 0.45 eV compared with the HOMO energy levels of the other three polymers, which reduced the band gap of PDTP-DTQx.

Photovoltaic Properties. Bulk heterojunction type PSCs were fabricated with a conventional sandwich structure, where the active layer was composed of one of the DTQx-based polymers as the donor and a fullerene derivative (either PCBM or PC$_{70}$BM) as the acceptor. The devices were optimized by changing many conditions, such as the ratio of the donor and the acceptor, the thickness of blend films, the solvent, the thermal annealing temperature and the cathode metal. For the polymer:PCBM systems, using Al as the cathode and postdeposition annealing at 110 °C for 5 min gave the best device performance. On the other hand, the highest PCEs were achieved by using Ca/Al as cathode and without postdeposition annealing for the polymer:PC$_{70}$BM systems.

Figure 4 shows the *I*−*V* curves of the optimized devices based on each of the DTQx-based polymers under illumination of AM 1.5 simulated solar light (100 mW/cm^2). The corresponding V_{OC}, short-circuit current (I_{SC}), fill factor (FF), and PCE of the devices are summarized in Table 2.

The device based on PF-DTQx:PCBM spin-coated from CB had PCE of 1.75%. Use of the mixture solvent of CB and CF (2:1 by volume) for the same component increased the PCE to 2.78%. Use of PC$_{70}$BM as acceptor further improved the efficiency to 3.23%. This large enhancement of the photovoltaic performance could be attributed to the change in the morphology of the blend film.[19g] Atomic force microscopy (AFM) images (Figure 5) clearly show large domains with a size of ~100 nm in the blend films prepared from CB. This would diminish exciton migration to the donor/acceptor interface and would be unfavorable for charge separation. The morphology of the blend films of both PF-DTQx:PCBM

---

(21) (a) Sun, Q. J.; Wang, H. Q.; Yang, C. H.; Li, Y. F. *J. Mater. Chem.* **2003**, *13*, 800. (b) Zhou, E. J.; Tan, Z. A.; Yang, C. H.; Li, Y. F. *Macromol. Rapid Commun.* **2006**, *27*, 793. (c) Zhou, E. J.; Tan, Z. A.; Huo, L. J.; He, Y. J.; Yang, C. H.; Li, Y. F. *J. Phys. Chem. B* **2006**, *110*, 26062. (d) Zhou, E. J.; He, C.; Tan, Z. A.; Yang, C. H.; Li, Y. F. *J. Polym. Sci., Part A: Polym. Chem.* **2006**, *44*, 4916. (e) Zhou, E. J.; Tan, Z. A.; Yang, Y.; Huo, L. J.; Zou, Y. P.; Yang, C. H.; Li, Y. F. *J. Macromolecules* **2007**, *40*, 1831.

Table 2. Device Characteristics of PSCs Based on the DTQx-Based Polymers in Combination with PCBM or $PC_{70}BM$

polymer:acceptor (w/w)		solvent	V_{OC} (V)	I_{SC} (mA/cm^2)	FF	PCE (%)
PF-DTQx (1:4)	PCBM	CB	0.86	4.77	0.43	1.75
	PCBM	CB:CF = 2:1	0.86	5.75	0.56	2.78
	$PC_{70}BM$	CB:CF = 2:1	0.86	6.75	0.55	3.23
PC-DTQx (1:3)	PCBM	CB	0.76	4.49	0.42	1.43
	$PC_{70}BM$	CB	0.76	7.26	0.40	2.20
PIC-DTQx (1:4)	PCBM	CB	0.84	3.86	0.48	1.56
	$PC_{70}BM$	DCB	0.80	7.38	0.43	2.54
PDTP-DTQx (1:2)	PCBM	CB	0.46	5.25	0.48	1.17
	$PC_{70}BM$	DCB	0.46	7.78	0.49	1.77

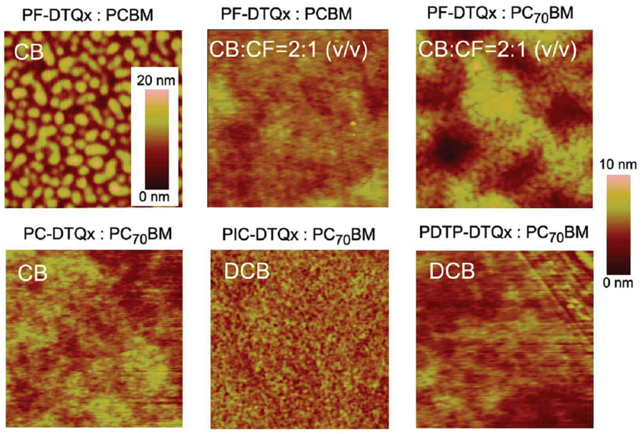

Figure 5. AFM height images of four DTQx-based polymers with PCBM or $PC_{70}BM$ composite films, spin-coated from different solutions (image size: 2 μm × 2 μm).

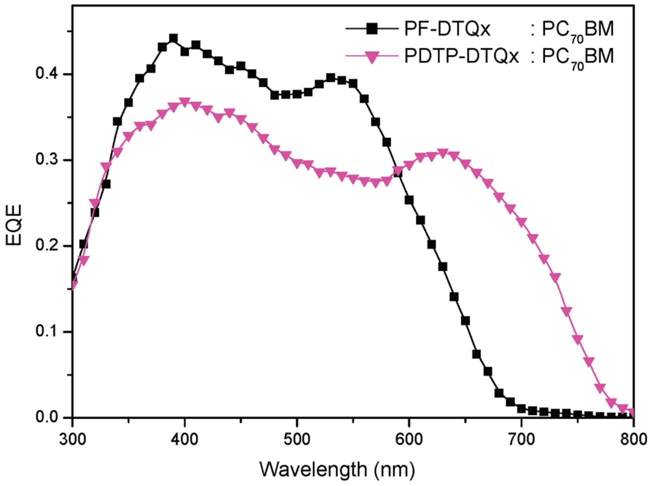

Figure 6. EQE plots of PSCs based on PF-DTQx:$PC_{70}BM$ and PDTP-DTQx:$PC_{70}BM$.

and PF-DTQx:$PC_{70}BM$ prepared from the mixture of CB and CF was much more uniform, without extensive phase separation.

For the other three polymers, uniform blend morphology was obtained merely by using suitable solvents. The AFM images of PC-DTQx:$PC_{70}BM$ film spin-coated from CB and PIC-DTQx:$PC_{70}BM$ and PDTP-DTQx:$PC_{70}BM$ films spin-coated from DCB are also shown in Figure 5. In the optimized conditions, the DTQx-based polymers showed PCEs in the range of 1.17−3.23%; these PCEs are comparable with those of the corresponding DTBT-based polymers. When PCBM was used as the electron acceptor, the PCEs of PSCs based on PF-DTBT, PC-DTBT, PIC-DTBT, and PDTP-DTBT were 2.67, 3.05, 1.47, and 2.18%, respectively.[12,20] The donor segment that gives the highest performance depends on the acceptor segment (carbazole for DTBT and fluorene for DTQx), revealing the complexity of choosing the proper D−A combination for PSCs.

Figure 6 shows the external quantum efficiency (EQE) plots of the optimized PSC devices with PF-DTQx:$PC_{70}BM$ and PDTP-DTQx:$PC_{70}BM$ under the illumination of monochromatic light. In both cases, the shape of the EQE plot is similar to the absorption spectrum of the device, indicating that all the absorption wavelengths of the polymers contributed to photocurrent generation. Comparing the EQE plots and the absorption spectra of the polymers in Figure 2, we can see that $PC_{70}BM$ absorption contributes substantially to the photocurrent by filling the valley of the polymer absorption. As a result, the EQE of the device with PF-DTQx:$PC_{70}BM$ covers most of the visible wavelength range from 300 to 700 nm, and in the case of PDTP-DTQx:$PC_{70}BM$, the EQE response extends to 770 nm.

Conclusion

The combination of DTQx with four types of donor segments in D−A type semiconducting polymers was investigated for application to PSCs. The photovoltaic properties of PSCs based on the four DTQx-based polymers and PCBM or $PC_{70}BM$ were evaluated, and a maximum PCE of 3.23% was achieved with PF-DTQx by optimizing the conditions of device fabrication. The results demonstrate that DTQx is a promising building block that can be combined with many donor segments to design efficient D−A type photovoltaic polymers.

Experimental Section

Synthesis. All the chemicals were purchased from Alfa, Aldrich or Wako and used without further purification. The following compounds were synthesized according to procedures in the literature:

5,8-di(2-bromothien-5-yl)-2,3-diphenylquinoxaline (monomer **3**),[19] 2,7-bis-(4,4,5,5-tetramethyl-1,3,2-dioxaborolan-2-yl)-N-[1-(2′-ethylhexyl)-3-ethylheptanyl]carbazole (monomer **5**),[7] 3,9-bis(4,4,5,5-tetramethyl-1,3,2-dioxaborolan-2-yl)-5,11-di(1-decylundecyl)-indolo[3,2-b]carbazole (monomer **6**),[13] and 2,6-di(trimethyltin)-N-[1-(2′-ethylhexyl)-3-ethylheptanyl]-dithieno[3,2-b:2′,3′-d]pyrrole (monomer **7**).[12]

Synthesis of Poly{9,9-dioctylfluorene-2,7-diyl-*alt*-5,8-dithien-2-yl-2,3-diphenylquinoxaline-5′,5″-diyl} (PF-DTQx). Monomer **3** (230 mg, 0.38 mmol), monomer **4** (223 mg, 0.4 mmol), and Aliquat 336 (~50 mg) were dissolved in a mixture of toluene (20 mL) and a 2 M aqueous solution of Na_2CO_3 (12 mL). The reaction vessel was purged with N_2 for 30 min to remove O_2. $Pd(PPh_3)_4$ (2%, 9 mg) was added, and the reaction mixture was heated under reflux overnight (~12 h). Phenylboronic acid (100 mg in 1 mL THF) was added, and after 2 h, bromobenzene (1 mL) was added. The mixture was allowed to reflux for 2 h and cooled to room temperature. The polymer was precipitated by slowly pouring the mixture into MeOH, filtered and Soxhlet extracted with MeOH, hexane, and $CHCl_3$. The $CHCl_3$ solution was passed through a column packed with alumina, Celite, and silica gel. The column was eluted with $CHCl_3$. The combined polymer solution was concentrated and poured into MeOH. The precipitate was then collected and dried under vacuum overnight. Yield: 170 mg (51%). ^{1}H NMR ($CDCl_3$, 400 MHz): δ (ppm) 8.2−7.4 (m, 22H), 2.12 (br, 4H), 1.2−0.7 (m, 30H). M_n = 8.1 k; polydispersity = 1.7.

Synthesis of Poly{*N*-[1-(2′-ethylhexyl)-3-ethylheptanyl]carbazole-2,7-diyl-*alt*-5,8-dithien-2-yl-2,3-diphenylquinoxaline-5′,5″-diyl} (PC-DTQx). PC-DTQx was prepared using the procedure for the synthesis of PF-DTQx, but monomer **3** (172 mg, 0.285 mmol) and monomer **5** (197 mg, 0.3 mmol) were used as starting materials. Yield: 150 mg (62%). ^{1}H NMR ($CDCl_3$, 400 MHz): δ (ppm) 8.2−7.3 (m, 22H), 4.85 (br, 1H), 2.49 (br, 2H), 1.81 (br, 2H), 1.4−0.7 (m, 30H). M_n = 10.5 k; polydispersity = 1.9.

Synthesis of Poly{5,11-di(1-decylundecyl)indolo[3,2-b]carbazole-3,9-diyl-*alt*-5,8-dithien-2-yl-2,3-diphenylquinoxaline-5′,5″-diyl} (PIC-DTQx). PIC-DTQx was prepared using the procedure for the synthesis of PF-DTQx, but monomer **3** (157 mg, 0.26 mmol) and monomer **6** (285 mg, 0.26 mmol) were used as starting materials. Yield: 230 mg (90%). ^{1}H NMR ($CDCl_3$, 400 MHz): δ (ppm) 8.4−7.3 (m, 24H), 4.75 (br, 2H), 2.50 (br, 4H), 2.05 (br, 4H), 1.4−0.9 (m, 76H). M_n = 21.1 k; polydispersity = 1.6.

Synthesis of Poly{*N*-[1-(2′-ethylhexyl)-3-ethylheptanyl]-dithieno-[3,2-*b*:2′,3′-*d*]pyrrole-2,6-diyl-*alt*-5,8-dithien-2-yl-2,3-diphenylquinoxaline-5′,5″-diyl} (PDTP-DTQx). Monomer **3** (249 mg, 0.412 mmol), monomer **7** (306 mg, 0.412 mmol), and dry toluene (20 mL) were added to a 50 mL double-neck round-bottom flask. The reaction vessel was purged with N_2 for 30 min to remove O_2. $Pd(PPh_3)_4$ (3%, 14 mg) was added, and the mixture was heated to 110 °C. The solution was stirred at 110 °C for 48 h. The dark blue sticky solution was cooled to room temperature and poured into MeOH. The precipitates were collected by filtration and washed with MeOH. The solid was dissolved in $CHCl_3$ (150 mL) and passed through a column packed with alumina, Celite, and silica gel. The column was eluted with $CHCl_3$. The combined polymer solution was concentrated and poured into MeOH. The precipitates were collected and dried. Yield: 160 mg (45%). ^{1}H NMR ($CDCl_3$, 400 MHz): δ (ppm) 7.9−7.0 (m, 18H), 4.5 (br, 1H), 2.1−0.5 (m, 34H). M_n = 11.2 k; polydispersity = 1.4.

Characterization. ^{1}H NMR (400 MHz) spectra were measured on a JEOL Alpha FT-NMR spectrometer equipped with an Oxford superconducting magnet system. Gel permeation chromatography (GPC) was performed on a Shimadzu Prominence system equipped with a UV detector(eluent: chloroform; 40 °C). The chloroform solution was filtered through a PTFE filter (pore size: 1.0 μm) before sample injection. UV−vis spectra were recorded on a JACSO V-650 spectrometer. Cyclic voltammograms (CVs) were recorded with an HSV-100 (Hokuto Denkou) potentiostat. A Pt plate coated with a thin polymer film was used as the working electrode. A Pt wire and an Ag/Ag^+ (0.01 M of $AgNO_3$ in acetonitrile) electrode were used as the counter and reference electrodes (calibrated vs Fc/Fc^+), respectively. AFM measurements were carried out on a Digital Instrumental Nanoscope 31 operated in tapping mode.

Fabrication and Characterization of Polymer Solar Cell. PSCs were constructed in the typical sandwich structure through several steps. ITO-coated glass substrates were cleaned by ultrasonication sequentially in detergent, water, acetone, and 2-propanol. After drying the substrate, PEDOT:PSS (Baytron P) was spin-coated (4000 rpm for 30 s) onto ITO. The film was dried at 150 °C under N_2 atmosphere for 5 min. After cooling the substrate, a solution of the DTQx-based polymer and PCBM (or $PC_{70}BM$) mixture was spin-coated onto the substrate inside a nitrogen-filled glovebox. The substrate was annealed at 80 °C for 30 min to remove the solvent. For the polymer/PCBM system, an Al (30 nm) electrode was evaporated onto the substrate under high vacuum (1×10^{-4} to 1×10^{-5} Pa) in an evaporation chamber (ALS Technology H-2807 vacuum evaporation system with E-100 load lock). Postdeposition annealing was carried out at 110 °C for 5 min inside a nitrogen-filled glovebox. For the polymer/$PC_{70}BM$ system, a Ca/Al (20 nm/60 nm) electrode was used and without postdeposition annealing. The photovoltaic cells with no protective encapsulation were subsequently tested in air under simulated air mass (AM) 1.5 solar irradiation (100 mW cm^{-2}, Peccell Technologies PCE-L11). Light intensity was adjusted by using a standard silicon solar cell with an optical filter (Bunkou Keiki BS520). The current−voltage characteristics of the photovoltaic cells were measured on a Keithley 2400 I−V measurement system. The effective areas of the PSCs were defined using a metal photomask (2 mm ×3 mm) during the irradiation of the simulated solar light.[22]

---

(22) (a) Zhou, E. J.; Yamakawa, S.; Tajima, K.; Yang, C. H.; Hashimoto, K. *Chem. Mater.* **2009**, *21*, 4055. (b) Zhou, E. J.; Tajima, K.; Yang, C. H.; Hashimoto, K. *J. Mater. Chem.* **2010**, *20*, 2362. (c) Zhou, E. J.; Wei, Q. S.; Yamakawa, S.; Zhang, Y.; Tajima, K.; Yang, C. H.; Hashimoto, K. *Macromolecules* **2010**, *43*, 821.